Bio-inspired sunlight-pumped lasers

Francesco Mattiotti,[1, 2, 3] William M. Brown,[4] Nicola Piovella,[5]
Stefano Olivares,[5, 6] Erik M. Gauger,[4] and G. Luca Celardo[7, *]

[1]*Department of Physics, University of Notre Dame, Notre Dame, IN 46556, USA*
[2]*Dipartimento di Matematica e Fisica and Interdisciplinary Laboratories for Advanced Materials Physics,
Università Cattolica, via Musei 41, Brescia I-25121, Italy*
[3]*Istituto Nazionale di Fisica Nucleare, Sezione di Pavia, via Bassi 6, Pavia I-27100, Italy*
[4]*SUPA, Institute of Photonics and Quantum Sciences,
Heriot-Watt University, Edinburgh, EH14 4AS, United Kingdom*
[5]*Dipartimento di Fisica "Aldo Pontremoli", Universit degli Studi di Milano, via Celoria 16, Milano I-20133, Italy*
[6]*Istituto Nazionale di Fisica Nucleare, Sezione di Milano, via Celoria 16, Milano I-20133, Italy*
[7]*Benemérita Universidad Autónoma de Puebla, Apartado Postal J-48, Instituto de Física, 72570, Mexico*
(Dated: July 9, 2020)

Even though sunlight is by far the most abundant renewable energy source available to humanity, its dilute and variable nature has kept efficient ways to collect, store, and distribute this energy tantalisingly out of reach. Turning the incoherent energy supply provided by the Sun into a coherent laser beam would overcome several of the practical limitations inherent in using sunlight as a source of clean energy: laser beams travel nearly losslessly over large distances, and they are effective at driving chemical reactions which convert sunlight into chemical energy. Here we propose a bio-inspired blueprint for a novel type of laser with the aim of upgrading unconcentrated natural sunlight into a coherent laser beam. Our proposed design constitutes an improvement of several orders of magnitude over existing comparable technologies: state-of-the-art solar pumped lasers operate above 1000 suns (corresponding to 1000 times the natural sunlight power). In order to achieve lasing with the extremely dilute power provided by natural sunlight, we here propose a laser medium comprised of molecular aggregates inspired by the architecture of natural photosynthetic complexes. Such complexes, by exploiting a highly symmetric arrangement of molecules organized in a hierarchy of energy scales, exhibit a very large internal efficiency in harvesting photons from a power source as dilute as natural sunlight. Specifically, we consider substituting the reaction center of photosynthetic complexes in purple bacteria (*Rhodobacter Sphaeroides*) with a suitably engineered molecular dimer composed of two strongly coupled chromophores. We show that if pumped by the surrounding photosynthetic complex, which efficiently collects and concentrates solar energy, the core dimer structure can reach population inversion, and reach the lasing threshold under natural sunlight. The design principles proposed here will also pave the way for developing other bio-inspired quantum devices.

INTRODUCTION

One of the most remarkable aspects of many natural molecular aggregates is their ability to efficiently process extremely weak sources of energy or signals for biological purposes. Examples of this include the ability of avian magneto-receptors to sense the extremely weak geomagnetic field [1–4], or the ability of aquatic bacterial photosynthetic systems to harvest sunlight in deep murky waters, where incident light levels are much reduced beyond the already dilute level on land [5, 6]. For instance, purple bacteria have the ability to exploit extremely weak light sources [5, 6] (less than 10 photons per molecule per second) and some species of green sulfur bacteria even perform photosynthesis with geothermal radiation from deep-sea hydrothermal vents at about 400°C [7]. This incredible ability of bacterial photosynthetic systems to utilise weak sources of incoherent light stems from highly symmetric molecular aggregates organized in hierarchical structures which have evolved to harvest light and funnel the collected energy to specific molecular aggregates [8, 9]. In this Article, inspired by the design of the photosynthetic apparatus of purple bacteria [5, 6], we show that bio-mimetic molecular aggregates hold the promise of significantly lowering the threshold requirements for sunlight-pumped lasers.

Sunlight is by far the most abundant renewable energy source on Earth (a single hour of sunlight provides all the energy humanity uses in a whole year). Despite this, there remain significant limitations in utilising sunlight as it is both dilute and variable. Therefore, efficient storage and distribution of energy harvested from sunlight is paramount. In this respect, sunlight-pumped lasing is an extremely promising technology for energy harvesting, distribution and storage of solar energy [10]. Sunlight-pumped lasers transform natural incoherent sunlight into intense beams of coherent light, which can be used to efficiently distribute the collected energy and drive chemical reactions as a way to efficiently store solar energy. Indeed, sunlight-pumped lasers have been proposed as essential elements in several renewable energy technologies such as the magnesium cycle [11–13].

Since the power density in natural sunlight is very di-

lute, typically concentrated sunlight is needed to cross the lasing threshold. Experimentally, a concentration of 10^5 'suns' (1 sun = 0.14 W/cm^2) is reachable, but clearly the smaller the 'number of suns' required for reaching the lasing threshold the better, since this lowers cost, technical demand, and increases efficiency. The first sunlight-pumped laser was realized in 1963 [10] and current state-of-the-art sunlight-pumped lasers operate above 1000 suns [14], however, proposals for sunlight-pumped lasers operational at few hundreds suns have been developed [14]. Typically, the concentration of sunlight relies on imaging or non-imaging concentrators. One of the most efficient way to concentrate sunlight is through black-body cavity pumping, where concentrated sunlight collected by a mirror heats a black-body cavity to temperatures which range from 1000 K to 3000 K [10].

Inspired by natural photosynthetic complexes, we propose a bio-mimetic molecular architecture to achieve efficient sunlight-pumped lasers capable of operating at pumping intensities as low as 1 sun. Photosynthetic antenna complexes [5, 6, 15–22] are comprised of a network of chlorophyll molecules which are typically modelled as two-level systems (2LS) capable of absorbing radiation and transporting the resulting electronic excitation to the reaction center where charge separation occurs, a process which precedes and drives all other photosynthetic steps. Each 2LS has an associated transition dipole moment (TDM) which determines its coupling with both the electromagnetic field and also with other proximal chlorophyll molecules. Owing to the low solar photon density, photosynthetic aggregates operate in the single-excitation regime, meaning at most one excitation is present in the system at any one time. The design principles which allow natural photosynthetic complexes to be so efficient rely on several levels of organization. On the lower level, single molecular aggregates feature a high degree of symmetry which favours the formation of bright (superradiant) or dark (subradiant) states with, respectively, large or small dipole strength [5, 6, 20, 23]. On a higher level, photosynthetic systems assemble many of these symmetric aggregates into hierarchical structures to maximize light-harvesting and energy transport. For instance, in purple bacteria, symmetric rings of chlorophyll molecules (LHI and LHII) surround the reaction center. These rings are J-aggregates with superradiant bright states which favor the absorption of light and the transfer of the excitation between each other [5, 6].

Many molecular aggregates, both naturally occurring as well as artificially synthesized, display bright and dark states in their single-excitation manifold [24–27]: J-aggregates are characterized by a bright state below the energy of the monomer absorption peak, while H-aggregates are characterized by a bright state above the energy of the monomer absorption peak. Cooperative properties, such as those seen in photosynthetic aggregates, have inspired many proposals for engineering artificial light-harvesting devices [28–35]. The lasing properties of molecular aggregates, such as organic crystals

(3D molecular aggregates) which display strong cooperative effects in the form of H- or J-aggregates, have been widely investigated [36–38].

Our proposed bio-inspired molecular architecture has at its core a suitably engineered molecular H-dimer. In an H-dimer the interaction between the excited states of each molecules create a bright state at high energy and a dark state at low energy. Under illumination, energy is absorbed mainly by the bright high-energy state and quickly transferred by thermal relaxation to the lower-energy state, which, being dark, loses energy by re-emission very slowly. Thus, an H-dimer is an ideal candidate to achieve population inversion (which is a main requirement for lasing) and its lower dark excitonic state can be exploited for the lasing transition. Nevertheless, natural sunlight is so weak that the required level of darkness of the lower excitonic state to achieve lasing would be unrealistically high. Indeed, the very long required excitonic lifetime of the lowest-excited state in the single-excitation manifold might be difficult to achieve in practice, due to disorder and competing non-radiative decay processes. In order to increase the pumping on the bright dimer state, so that the requirement on the darkness of the lower excitonic state can be relaxed, we consider substituting the reaction center of photosynthetic complexes in purple bacteria "Rhodobacter Sphaeroides" with a suitably engineered H-dimer [playing a role similar to the special pair in the reaction center [5, 6]]. Indeed, natural antenna systems are extremely efficient precisely at collecting and funneling natural sunlight energy to specific locations. We show that a randomly positioned ensemble of such molecular aggregates inside a double-mirror cavity can lase under weak black-body radiation pumping (delivered by a surrounding black-body cavity that is heated by concentrated sunlight), even under natural sunlight illumination.

We proceed by first deriving lasing equations for a generic molecular aggregate. We then consider lasing from an ensemble of isolated H-dimers. We show that placing the H-dimer at the center of a purple bacteria LHI ring lowers the lasing threshold and allows for less restrictive requirements on the darkness of the subradiant state of the H-dimer, with further advantages when adding additional LHII rings as occurs in the natural template. While we mainly focus on an aggregate inspired by photosynthetic apparatus of purple bacteria, we also consider a molecular architecture inspired by the photosynthetic complex of green sulfur bacteria [39] in the Supporting Information (SI).

LASING EQUATIONS FOR MOLECULAR AGGREGATES

We begin with the derivation of lasing equations for a generic ensemble of molecular aggregates, each made of N identical molecules, that are placed in an optical lasing cavity with suitably chosen frequency. The Hamiltonian

of the molecular aggregate is written with the usual Pauli operators as

$$\hat{H}_S = \sum_{j=1}^{N} \frac{\hbar\omega_A}{2}\hat{\sigma}_j^z + \sum_{i,j} \Omega_{i,j}\left(\hat{\sigma}_i^+\hat{\sigma}_j^- + \hat{\sigma}_j^+\hat{\sigma}_i^-\right) , \quad (1)$$

where $\Omega_{i,j} = (\vec{\mu}_i \cdot \vec{\mu}_j)/r_{ij}^3 - 3(\vec{\mu}_i \cdot \vec{r}_{ij})(\vec{\mu}_j \cdot \vec{r}_{ij})/r_{ij}^5$ is the dipolar inter-molecular coupling [23, 40, 41] with $\vec{\mu}_j$ being the TDM of the j-th molecule in the aggregate and $\vec{r}_{ij}$ the vector between the i-th and the j-th molecule[42]. Equation (1) represents a molecular aggregate where each molecule is approximated as a 2LS with splitting ω_A. Under the relatively weak pumping conditions considered here, rather than retaining the full Hilbert space of dimension 2^N it suffices to limit our analysis to the overall aggregate ground state $|G\rangle$ and the single-excitation manifold comprised of N states $|j\rangle$ where the j-th molecule is excited while all the other ones are in their respective ground states.

We capture thermal relaxation by coupling each molecule to an independent bath of harmonic oscillators, and for simplicity we here neglect vibronic effects [27]. The interaction of the molecular aggregate with black-body radiation and phonons is then governed by the master equation

$$\frac{d\hat{\rho}(t)}{dt} = -\frac{i}{\hbar}\left[\hat{H}_S, \hat{\rho}(t)\right] + \mathcal{D}_{BB}[\hat{\rho}(t)] + \mathcal{D}_T[\hat{\rho}(t)], \quad (2)$$

where $\mathcal{D}_{BB}$ and $\mathcal{D}_T$ are the Bloch-Redfield dissipators for the coupling to the black-body cavity and phonon environments, respectively (see SI). In our simulations phonon bath parameters have been chosen in order to effect thermal relaxation within few picoseconds, typical of molecular aggregates [5, 6].

Equation (2) can be largely simplified under well-motivated assumptions: first, as we check and validate numerically in the SI, we may safely secularise and reduce our master equation to Lindblad form [43]. Moreover, since thermal relaxation is typically the fastest time scale for molecular aggregates at room temperature (RT), we can assume that the populations in the single-excitation manifold are always at thermal equilibrium. Let us define the total probability for the aggregate to be excited as $P_e = \sum_k P_k$, where P_k is the probability of the $|k\rangle$ single excitation eigenstate to be excited. Neglecting higher excitation manifolds, we write $P_G + P_e = 1$, where P_G is the probability to be in the ground state. Then, assuming thermal equilibrium, we have

$$P_k = P_e p_k \quad \text{with} \quad p_k = \frac{e^{-E_k/k_B T}}{\sum_n e^{-E_n/k_B T}}, \quad (3)$$

where E_k is the energy of the k-th excitonic eigenstate, and we assume henceforth $T = 300$ K.

The coupling with the black-body photon bath is well-approximated by rate equations for the populations (see SI and Ref. [44]), with absorption rates between the $|G\rangle$

and the single-excitation states $|k\rangle$ given by

$$R_k = n_T^k \gamma_k, \quad \text{with} \quad \gamma_k = \frac{\mu_k^2 \omega_k^3}{3\pi\epsilon_0\hbar c^3}$$
$$\text{and} \quad n_T^k = \frac{1}{e^{E_k/k_B T_{BB}} - 1}, \quad (4)$$

where γ_k is the spontaneous decay rate of the k-th state, ω_k and μ_k its transition frequency and TDM, respectively, and n_T^k the photon occupancy at the black-body temperature T_{BB}.

As our laser gain medium, we consider an ensemble of molecular aggregates randomly distributed with density n_A inside a lasing cavity of frequency ω_c and containing a classical oscillating field $\vec{E} = E_0\hat{\epsilon}\cos(\omega_c t)$. The aggregate's single-excitation states $|k\rangle$ couple coherently to the cavity mode with Rabi frequencies $\Omega_k = (\vec{\mu}_k \cdot \hat{\epsilon})E_0/\hbar$ that depend on the cavity polarization $\hat{\epsilon}$ and field amplitude E_0. In molecular aggregates under weak pumping, the Rabi frequency is typically smaller than the interband excitonic dephasing rate, $\Gamma_\phi \gg \Omega_k$. Therefore, instead of coherent Rabi oscillations we obtain incoherent transition rates proportional to Ω_k^2, as derived in the SI and Ref. [45]. The field intensity $I = \epsilon_0|E_0|^2 c/2$ can also be written as $I = \hbar\omega_c nc/V$, where n is the number of photons in the cavity, V the cavity volume, and c the speed of light. This allows us to express the cavity-induced transition rate between $|G\rangle$ and $|k\rangle$ state in terms of the number of cavity photons n as

$$nB_k = n\frac{1}{3}\frac{|\mu_k|^2\omega_c}{V\hbar\epsilon_0}\frac{\Gamma_\phi}{\Gamma_\phi^2 + (\Delta_k/\hbar)^2} = \frac{\Omega_k^2}{2}\frac{\Gamma_\phi}{\Gamma_\phi^2 + (\Delta_k/\hbar)^2}, \quad (5)$$

where $\Delta_k = (E_k - \hbar\omega_c)$ is the energy detuning between the single-excitation state k and the cavity mode. The factor $1/3$ derives from averaging over the random aggregate orientations.

Under the above assumption we can write lasing rate equations that couple the populations of the molecular aggregates with the number of photons in the cavity. For this purpose, let us define the density of aggregates in the excited states as $N_e = n_A P_e$, the density of aggregates in the ground state as $N_G = n_A P_G$, and the population difference per unit volume as $D = N_e - N_G$. This gives the lasing equations

$$\frac{dD}{dt} = -D[R_d + R_u + (B_{tot} + \langle B\rangle)n] + \\ + n_A[R_u - R_d + n(B_{tot} - \langle B\rangle)] \quad (6a)$$

$$\frac{dn}{dt} = V(B_{tot} + \langle B\rangle)\frac{nD}{2} - V(B_{tot} - \langle B\rangle)\frac{nn_A}{2} - \kappa n, \quad (6b)$$

where $R_u = \sum_k R_k$ is the total absorption rate and $R_d = \sum_k(R_k + \gamma_k)p_k$ is the spontaneous and stimulated emission rate from the single-excitation manifold. Further, $B_{tot} = \sum_k B_k$ and $\langle B\rangle = \sum_k B_k p_k$ are, respectively, the total upwards and downwards transition rates

between $|G\rangle$ and the single-excitation manifold which is induced by the coupling to the cavity mode.

From (6) we obtain the stationary values of the population difference per unit volume D_0 and the stationary number of photons n_0 in the cavity

$$D_0 = \frac{2\kappa}{V(B_{tot} + \langle B \rangle)} + n_A \bar{B} \ , \qquad (7a)$$

$$n_0 = \frac{V(n_A D_{eq} - D_0)}{2\kappa}(R_u + R_d) \ , \qquad (7b)$$

where $\bar{B} = (B_{tot} - \langle B \rangle)/(B_{tot} + \langle B \rangle)$ and $D_{eq} = (R_u - R_d)/(R_u + R_d)$ is the equilibrium population difference in absence of driving from the cavity. Above the lasing threshold, i.e. having $n_0 > 0$ stationary photons in the cavity, the laser intensity and output power will be, respectively,

$$I = \frac{\hbar\omega_c c}{V}n_0 \ , \qquad (8a)$$

$$P_{out} = \frac{\kappa V}{c}I = \kappa\hbar\omega_c n_0 \ . \qquad (8b)$$

We turn to the question under which conditions we achieve lasing. Imposing $n_0 > 0$ in (7) we require $n_A D_{eq} - D_0 > 0$, which can be written as

$$n_A(D_{eq} - \bar{B}) > \frac{2\kappa}{V(B_{tot} + \langle B \rangle)} \ . \qquad (9)$$

Using the definitions of R_u and R_d and for $n_T^k \ll 1$,

$$D_{eq} \approx \frac{\sum_k \chi_k n_T^k - \langle \chi \rangle}{\sum_k \chi_k n_T^k + \langle \chi \rangle} \ , \qquad (10)$$

where $\chi_k = \gamma_k/\gamma_0$ indicates the relative brightness of the state $|k\rangle$ and $\langle \chi \rangle = \sum \chi_k p_k$ is the thermal average of the relative decay rates of all the single-excitation states. Moreover, $\gamma_0 = (\mu^2\omega_A^3)/(3\pi\epsilon_0\hbar c^3)$ is the spontaneous decay rate of a single molecule. We reiterate that Eq. (10) is generically valid subject to fast thermal relaxation and with negligible occupation of states containing more than one excitation. Both assumptions are realistic for molecular aggregates under black-body radiation pumping.

Equation (9) determines the critical density of molecular aggregates to achieve lasing, implying

$$D_{eq} > \bar{B} \ . \qquad (11)$$

Since $\bar{B} \geq 0$ by definition, unsurprisingly we require population inversion, $D_{eq} > 0$, to achieve lasing. Considering (11) with (10) and recalling that $R_u = \gamma_0 \sum_k \chi_k n_T^k$, implies $\langle \chi \rangle \leq \frac{R_u}{\gamma_0}\frac{1-\bar{B}}{1+\bar{B}}$, which can be recast as:

$$\langle \chi \rangle \leq \frac{R_u}{\gamma_0}\frac{\langle B \rangle}{B_{tot}} \ . \qquad (12)$$

Equation (12) clearly shows that given a non-zero (but realistically small) value for $\langle \chi \rangle$, two conditions need to be met for lasing: (i) the ratio $\langle B \rangle/B_{tot}$ should be as

large as possible, given $\langle B \rangle \leq B_{tot}$ this is maximized for $\langle B \rangle \approx B_{tot}$. This condition can be realised by a lasing state that is well-gapped (w.r.t. $k_B T$ at RT) below all other states in its excitation manifold; (ii) the absorption rate R_u should be as large as possible. Lasing under very weak pumping requires a highly dark aggregate (i.e. small $\langle \chi \rangle$), even if $\langle B \rangle \approx B_{tot}$. This is not easy to achieve, and the situation is compounded by non-radiative losses typically present in molecular aggregates. As we shall show in the following, a bio-inspired molecular architecture can help to mitigate this stringent demand and make lasing achievable.

Throughout this Article, when considering black-body optical pumping, we choose a temperature $T_{BB} = 3000$ K which is attainable using sunlight concentrated by a mirror of a few m^2 [10] with an input power into the black-body cavity of few kW. To compute the laser output power we assume a typical gain medium volume of $V = 11.3$ cm^3 (radius of 6 mm and length of 10 cm). The densities of the laser medium are chosen to be lower than 1 aggregate/(10 nm)^3, corresponding to realistic densities for dye lasers: $n_A^{(\max)} = 10^{18}$ cm$^{-3} = 1.6$ mmol/L [46]. This choice ensures that direct interactions between the molecular aggregates can be neglected. Moreover, it also keeps the output power below 1 kW, so that thermal balancing with the black-body cavity under realistic sunlight pumping can be maintained. To remove the need for and complexity of sunlight concentration we shall also consider the possibility to achieve lasing under direct natural sunlight illumination. To model natural sunlight we consider pumping under a black-body at $T_{BB} \approx 5800$ K but with rates in (4) reduced by a factor f_S representing the solid angle of the Sun as seen on Earth [47],

$$f_S = \frac{\pi r_S^2}{4\pi R_{ES}^2} = 5.4 \times 10^{-6} \ , \qquad (13)$$

with r_S being the radius of the Sun and R_{ES} the Sun-to-Earth distance. In this case we limit the output power to 1 W since the incident power on our chosen lasing cavity is just a few W.

LASING WITH DIMERS

Let us consider a dimer comprising two identical chromophores. Each molecule (labeled $j = 1, 2$) has one relevant optical transition, so that we may model it as a 2LS with ground state $|g_j\rangle$ and excited state $|e_j\rangle$. Excitation energy $\hbar\omega_A$ and magnitude μ of the electric TDM are identical between the molecules, while the direction of the optical dipole $\vec{\mu}_j$ depends on the orientation of its chromophores and may differ.

For this dimer system the Hamiltonian in (1) is diagonalized by a set of four states (see Fig. 1a): $|G\rangle = |g_1\rangle|g_2\rangle$, where both molecules are in their respective ground state; $|L\rangle$ and $|H\rangle$ are the lowest and highest single-excitation states, where only one excitation is
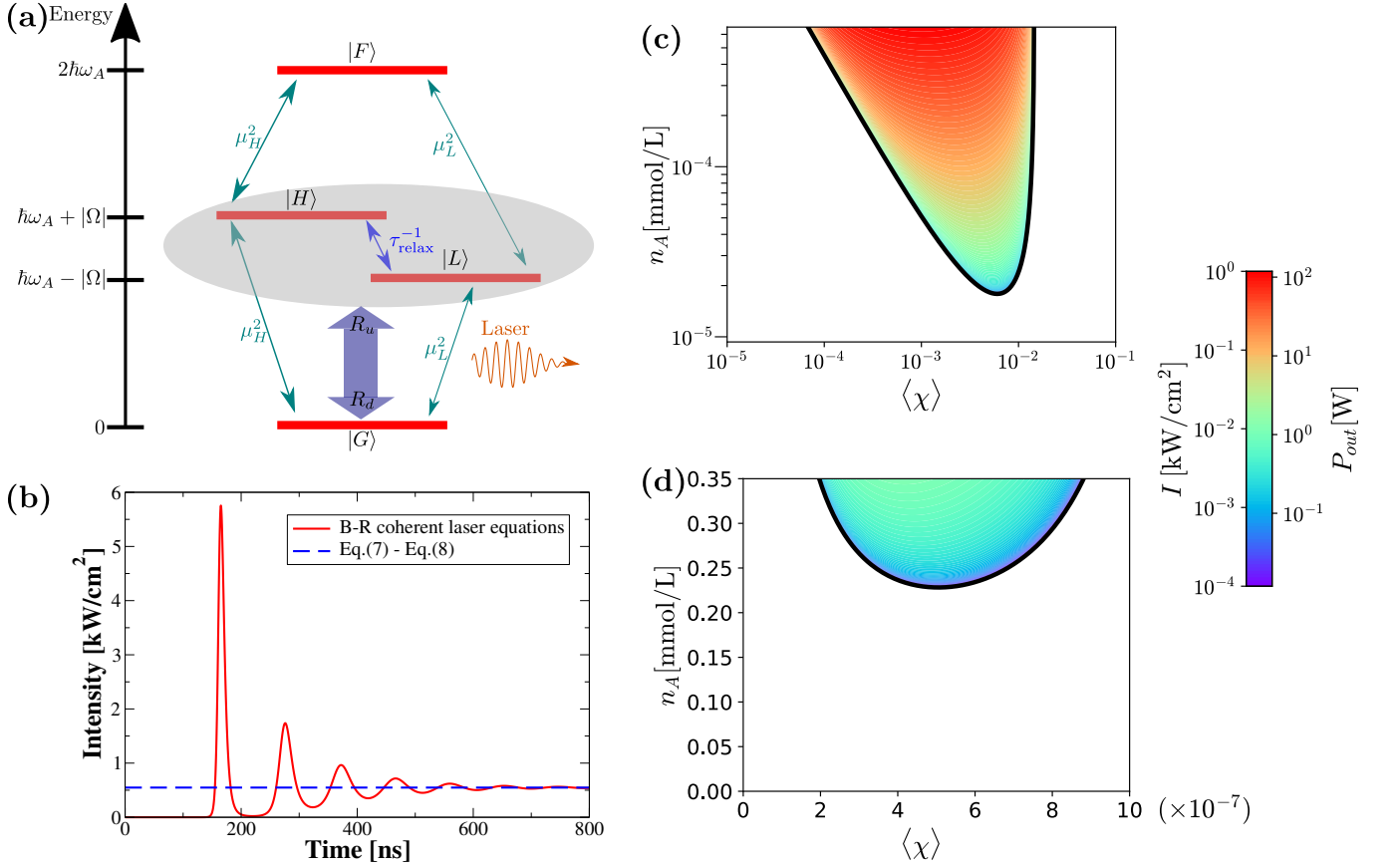
FIG. 1. **(a)** Eigenstates of the dimer Hamiltonian $\hat{H}_S$ (1) and transition rates between them. Optical rates (green arrows) are proportional to the squared dipole strengths [see (4)], while the thermal relaxation rate (blue arrow) is $\tau_{\rm relax}^{-1} \approx 1$ ps^{-1}. All these transitions obey detailed balance, i.e. upwards and downwards rates are proportional to the Bose-Einstein occupation number $n_T(\hbar\omega)$ and $[1 + n_T(\hbar\omega)]$, respectively. The thick double arrow represents the resulting effective rates linking the ground state $|G\rangle$ to the single-excitation manifold (grayed area), as utilised in Eq. (6a). The $|L\rangle - |G\rangle$ transition is further coupled to a resonant lasing cavity. **(b)** Temporal evolution of the laser intensity under black-body pumping: Bloch-Redfield model (solid red) for dimers that are coherently coupled to the lasing cavity (details in the SI), and steady-state solution (dashed blue) of our lasing equations, (7)-(8). Parameters: $\mu = 10.157$ D, $\hbar\omega_A = 1.17$ eV, $\Omega = 2000$ cm^{-1}, $T_{BB} = 3000$ K, $\Gamma_\phi = 1/(10$ ps), $\kappa/(2\pi) = 50$ MHz, $\langle\chi\rangle = 0.005$, $n_A = 5 \times 10^{-4}$ mmol/L, and a lasing cavity volume $V = 11.3$ cm^3 (cylindrical shape of radius $R = 6$ mm and length $L = 10$ cm). **(c)-(d)** Laser intensity and output power for the same parameters as (b) except for $\langle\chi\rangle$ (thermal average of the relative brightness of single-excitation states with respect to a single molecule) and n_A (dimer density in millimol/L) which are varied along the axes. The black line represents the lasing threshold [(9)]. In (c) optical pumping occurs via a black body radiation at $T_{BB} = 3000$ K, whereas in (d) the lasing medium is illuminated by natural sunlight.

present in the system, delocalised over both molecules; these states span the single-excitation manifold and they correspond to the symmetric and anti-symmetric states $(|g_1\rangle|e_2\rangle \pm |e_1\rangle|g_2\rangle)/\sqrt{2}$. Finally, $|F\rangle = |e_1\rangle|e_2\rangle$ has both molecules in their respective excited state. The corresponding energies are shown in Fig. 1a.

Optical transitions between the levels are determined by the relative orientation of the single molecules. We indicate the transition dipoles between the ground state $|G\rangle$ and the states $|L\rangle$ and $|H\rangle$ with $\vec{\mu}_L$ and $\vec{\mu}_H$, respectively, see Fig. 1a. The conservation of total oscillator strength demands that $\mu_L^2 + \mu_H^2 = \mu_1^2 + \mu_2^2 = 2\mu^2$ and we have an H-dimer if $\mu_L < \mu$ while if $\mu_L > \mu$ we have a J-dimer. The coupling Ω between molecules can either have a dipolar or a different origin, see SI. Typical H-

dimers feature splittings between their bright and dark states of several $k_B T$, and the lower state may be many hundreds times less bright than the upper state [24–27]. Here, we consider a dimer with excitation energy in the near-infrared $\hbar\omega_A = 1.17$ eV ($\lambda \approx 1060$ nm), transition dipole of $\mu = 10.157$ D (as for the bacteriochlorophyll-a molecule) and a coupling $\Omega = 2000$ cm^{-1} as in similar H-dimers [48].

Under black-body illumination, primarily the bright state $|H\rangle$ undergoes excitation, followed by rapid thermal relaxation to the lower dark $|L\rangle$ state. The large energetic separation between $|H\rangle$ and $|L\rangle$ makes this relaxation one-way, preventing environmental re-excitation into $|H\rangle$. In SI we show that it is possible to achieve population inversion provided the absorption rate $|G\rangle \to |H\rangle$

dominates over the spontaneous emission rate $|L\rangle \rightarrow |G\rangle$. We proceed to couple the $|L\rangle \rightarrow |G\rangle$ transition to a resonant lasing cavity and evaluate the lasing performance of the system using the equations derived in the previous section. Figure 1b shows the resulting laser intensity: once the stationary regime has been reached, there is perfect agreement between the intensity predicted by (6) with our numerically obtained results from a coherent Bloch-Redfield model. The latter, derived in Eqs. (S37, S43) of the SI, treats both photon and phonon environments in the Bloch-Redfield formalism, includes the doubly excited state, and – as its main assumption – treats the laser field semi-classically, but nonetheless coherently coupled to the aggregates similarly to Refs. [49, 50]. In Fig. 1c we show the dependence of the laser intensity and power output on n_A and $\langle\chi\rangle$ based on realistic choices for all other parameters (see caption). The white area highlights the region below the laser threshold (9) (black continuous line), where the dimer density n_A is too low to permit lasing. As one can see, an intensity of up to 1 kW/cm^2 can be reached with a very low dimer concentration.

To assess the possibility of lasing under direct natural sunlight illumination (i.e. without a black-body cavity heated by concentrated sunlight), we show the lasing threshold and output power for this scenario in Fig. 1d. Clearly, lasing is still theoretically possible but only for very low values of $\langle\chi\rangle$. In practice, this is challenging due to the competition of non-radiative decays and other sources of noise in realistic situations. Nevertheless, as we show in the next section, the critical value of $\langle\chi\rangle$ increases by orders of magnitude if the dimer is placed inside a purple bacteria molecular aggregate. Finally, note that for lasing we require a small yet finite value of $\langle\chi\rangle$. In the case of a homodimer (where for parallel TDMs the $|L\rangle$ dimer state would be fully dark) this can either arise as a consequence of the relative orientation of the TDMs, or through the presence of structural or energetic disorder.

BIO-INSPIRED LASERS

Whilst lasing with a gain medium composed of suitable H-dimers is realistic under black-body cavity pumping, achieving the extremely high optical darkness (small $\langle\chi\rangle$) for direct sunlight-pumped operation is a tall order. According to (12) $\langle\chi\rangle$ is upper-bounded by the pumping rate in units of γ_0 (assuming a favourable ratio $\langle B\rangle/B_{tot} \approx 1$). Thus increasing the effective pumping rate reduces the stringency of required darkness. A possible way of increasing pumping is to surround the dimer by a molecular aggregate that is capable of efficiently absorbing photons and transferring the resulting energy excitations to the $|H\rangle$ dimer state. The aggregate should absorb at an energy larger than the $|H\rangle$ dimer state energy in order to preserve the gap which separates the dimer lasing state from other states, so that $\langle B\rangle/B_{tot} \approx 1$. Note that un-

der this condition $\langle\chi\rangle$ of the whole aggregate can remain very close to $\langle\chi\rangle$ of the dimer alone. Here we consider a dimer surrounded by the antennae complex of purple bacterial photosynthetic systems that thrive in very low light intensity [5, 6, 8, 9, 52]. Moreover, in the SI a green sulfur bacteria antenna complex is used to increase the pumping of the dimer $|H\rangle$ state even further.

Purple bacteria feature a hierarchical structure of symmetric molecular aggregates which absorb light and direct the collected energy to the specific molecular aggregate of the reaction center (RC). The purple bacteria RC contains a bacteriochlorophyll (BChl) dimer called the special pair, and is surrounded by an LHI (Light-Harvesting system I) ring comprising 32 BChl molecules. The LHI ring is a J-aggregate with two superradiant states at 875 nm that are polarized in the ring plane and close to the lowest excitonic state. The LHI ring is surrounded by several LHII rings, each featuring the B850 ring, a J-aggregate composed of 18 BChl molecules with two superradiant states at 850 nm, and the B800 ring composed of 9 BChl molecules with main absorption peak at 800 nm. This hierarchical structure is able to absorb photons at different frequencies and guide the collected energy down an energetic funnel to the RC through a process dubbed supertransfer, resulting from the coupling between the LHII-LHI superradiant states and the LHI-RC aggregates [5, 6, 8, 9].

We propose substituting the special pair in the purple bacteria reaction center with an H-dimer whose $|H\rangle$ state is resonant with the superradiant states of LHI. Photons absorbed by the LHI ring would then contribute to the pumping of the dimer's $|H\rangle$ state, with the strong coupling between $|H\rangle$ and the bright state of the LHI complex ensuring fast transfer. The geometrical arrangement for this envisioned aggregate is shown in Fig. 2b [15, 16, 51, 52] (for full details see SI). Starting from a realistic model for the antenna system coupled to the dimer (see SI for details) we obtain the eigenvalues and the TDMs of all the energy states by direct Hamiltonian diagonalization, which allows evaluating the lasing equations (6) under the already discussed assumptions of negligible non-radiative losses and fast thermal relaxation. The latter is valid in this aggregate owing to supertransfer throughout the aggregate which entails thermal relaxation on the order of tens of picoseconds [15, 16]: this is much faster than optical pumping, which range from a few nanoseconds (large aggregates, high blackbody temperature) down to milliseconds (small aggregates, natural sunlight) and spontaneous decay, which is of the order of a nanosecond for the brightest states. Moreover, other relevant timescales are the transition rate due to the coupling to the lasing cavity field which we estimate to be larger than hundreds of picoseconds (for the parameters considered here), and the realistic extraction rate κ from the cavity of about three nanoseconds which we considered. In summary, thermal relaxation is clearly the fastest process, justifying the use of (6) for analyzing the lasing response of such bio-inspired
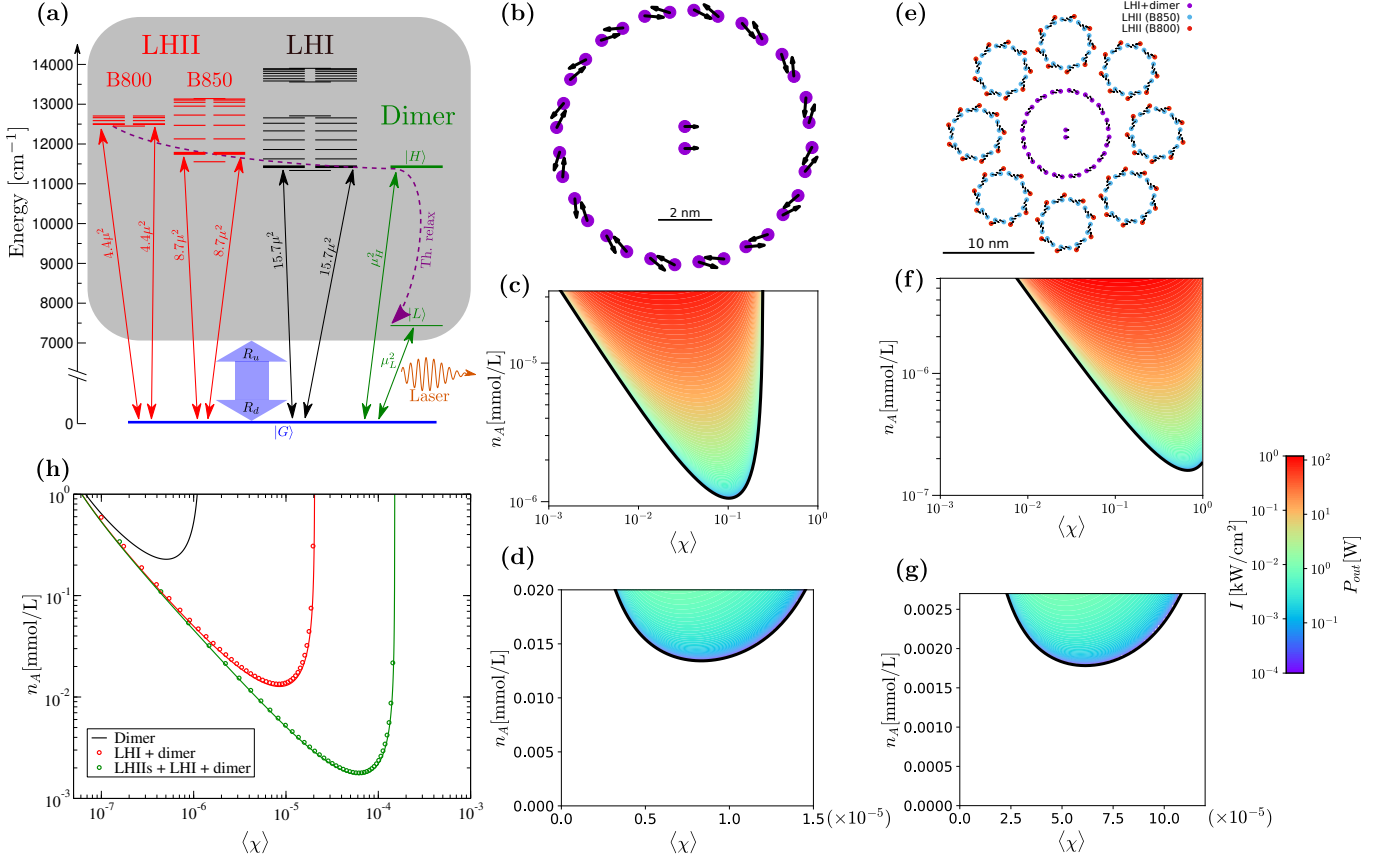
FIG. 2. **(a)** Single-excitation eigenstates of the LHII complex (with a distinction between the B800 and the B850 subunits), LHI complex, and H-dimer. The strongest optical rates, proportional to the squared dipole strengths, are indicated alongside the two-headed arrows. As before, the thick double arrow represents the resulting effective rates linking the ground state $|G\rangle$ to the single-excitation manifold (grayed area) and the $|L\rangle - |G\rangle$ dimer transition is also coupled to a lasing cavity. The H-dimer parameters are: $\mu = 10.157$ D, $\hbar\omega_A = 1.17$ eV, $\Omega = 2000$ cm^{-1}. Further, $\Gamma_\phi = 1/(10$ ps), $\kappa/(2\pi) = 50$ MHz, and $V = 11.3$ cm^3. **(b), (e)** Positions of the chromophores (circles) and transition dipole orientations (arrows) for the bio-mimetic complexes. Excitation energies and nearest-neighbour couplings for bio-mimetic aggregates are taken from Refs. [8, 15, 16, 51, 52]. **(c), (d), (f), (g)** Laser intensity and output power for an LHI ring surrounding an H-dimer (c,d) and with eight additional B800/850 LHII rings surrounding the LHI ring (f,g). On the axes we vary $\langle\chi\rangle$ of the H-dimer and n_A (the aggregate density in mmol/L). In all panels the black line represents the lasing threshold [(9)]. In (c,f) we have black-body pumping at temperature $T_{BB} = 3000$ K, whereas (d,g) are for natural sunlight illumination. **(h)** Lasing threshold density under natural sunlight for a bare dimer, one LHI surrounding the dimer as in (b), and eight LHIIs around an LHI ring containing the dimer as in (e). The red and green continuous curves are for a dimer with a re-scaled R_u pumping rate: by a factor of 17 (red curve) and by a factor of 125 (green curve), corresponding to an enhancement factor $N/2$ with N being the number of chromophores in the aggregate. The circles are obtained from the full set of optical transitions as indicated in (a).

aggregates. Moreover, in the SI, results of incoherent laser equations Eqs. (S62) in SI, which do not assume quasi-instantaneous thermalization, are shown to be in excellent agreement with (6).

The calculated lasing intensity and output power for a disordered ensemble of such aggregates (LHI+H-dimer) is shown in Fig. 2c for black-body cavity pumping, and in Fig. 2d for natural sunlight illumination. Comparing Fig. 1c-d with Fig. 2c-d, the critical aggregate density to cross the lasing threshold is greatly lowered, and more importantly, the required level of the dimer darkness for the natural sunlight case is reduced by more than an order of magnitude. We obtain a further improvement

when surrounding our LHI ring with eight LHII rings, see Fig. 2e. The B800/850 LHII aggregate level structure next to that of the LHI and H-dimer is shown in Fig. 2a. As shown in Fig. 2f-g this larger aggregate architecture achieves a further lowering of the lasing threshold, i.e. increase of the critical value of $\langle\chi\rangle$ for the H-dimer below which lasing is possible. Interestingly, in Fig. 2f, the addition of the rings has increased the effective pumping of the H-dimer to the extent where the dimer no longer has to feature a dark state to lase: indeed in this case lasing is possible even for $\langle\chi\rangle = 1$.

We have established that surrounding an H-dimer with purple bacteria LHI and LHII rings not only lowers the

necessary threshold density but also enables lasing with much less dark H-dimers. To better understand and visualise these trends, we map out the lasing transition as a function of threshold density and average brightness of the H-dimer for natural sunlight pumping in Fig. 2h[53]. This uses an H-dimer system described by (9) and (10) but with effective pumping R_u increased by the factor $N/2$, where N is the number of molecules in the bio-inspired aggregate including the H-dimer. This is a simplified approach of approximating enhanced pumping compared to the approach above based on the known TDMs of LHI/LHII states. Interestingly, the resulting threshold lines in Fig. 2h perfectly reproduce those obtained in the presence of the whole aggregate (symbols). This confirms that the crucial role of adding bio-inspired aggregates is to increase the effective pumping rate. Moreover, it suggests that our proposed architecture is scalable and an even lower lasing threshold could be achieved with larger J-aggregates surrounding the H-dimer, as we discuss in the SI, where we consider another bio-inspired architecture where the antenna complex of the green sulfur bacteria pumps the dimer $|H\rangle$ state. Nevertheless, caution is necessary when applying the lasing equations derived here to very large aggregates, where the assumption of thermalization occurring on the fastest relevant timescale can become invalid, in which case an incoherent laser equation might be more appropriate as discussed in SI.

CONCLUSIONS AND PERSPECTIVES

Efficient sunlight-pumped lasers could revolutionize renewable energy technologies, nevertheless lasing under natural sunlight illumination is still well beyond reach. By mimicking the architecture of photosynthetic antenna complexes, here we have shown how lasing with natural sunlight pumping can be achieved.

We first considered an ensemble of molecular H-dimers inside an optical cavity pumped by black-body cavity radiation. When considering realistic values of the H-dimer darkness, lasing is possible for high black-body temperatures which can be achieved by heating up a cavity with concentrated sunlight. Nevertheless, lasing with H-dimers under natural sunlight would require a very high level of darkness, which is very difficult to achieve. The main limitation is due to the very weak pumping produced by natural sunlight. Larger molecular H-aggregates might be able to lower the lasing threshold by absorbing more light and thus increasing the pumping. On the other hand, if not properly designed, large aggregates have an increased density of states which would suppress the thermal population of the lasing state. This effect would compete with the advantage gained by more absorbed light. In order to increase the absorbed light without suppressing the population of the lasing state, one possibility is to consider an aggregate which absorbs

light on a hierarchy of energy scales and which is able to efficiently funnel the absorbed energy to a low energy lasing state which is well-gapped below other excitonic states. In this way, its thermal population will not be suppressed. These are precisely the features which characterize many natural antenna photosynthetic systems. Our proposed bio-inspired molecular aggregate serving as the lasing medium is composed of an H-dimer operating at low energy, surrounded by LHI and LHII rings of the purple bacteria antenna complex, which absorb at higher energy and efficiently funnel the absorbed energy to the H-dimer. In this configuration, we show that lasing should be possible even under natural sunlight illumination.

The specific bio-inspired parameters we have analysed would implement a short wavelength infrared laser, which has the advantage of being able to efficiently distribute converted solar energy due to the low dispersion in this wavelength range [48], which is also why this spectral regime is used in optical fiber communications. As an interesting prospect, our bio-mimetic molecular aggregates should be able to lase in nanocavities with volume of $(\lambda/20)^3$ [54] and could thus be engineered into sun-light pumped nanolasers [55].

Our idea can be generalized to other bio-inspired molecular architectures where molecular (J-)aggregates efficiently pump the bright state of a homo-dimer; this would allow lasing in other spectral regimes, and utilising other photosynthetic systems, e.g. the chlorosome of green sulfur bacteria [56] (as discussed in SI) or photosynthetic membranes such as in Photosystem II [57] to feed excitations into $|H\rangle$ and make them available for the lasing transition.

ACKNOWLEDGMENTS

G.L.C. and F.M. conceived the study. N.P. and S.O. developed the semi-classical laser theory. G.L.C. and F.M. developed the incoherent laser equations and derived the laser equations presented in the main text. E.G. and W.B. developed the Bloch-Redfield master equation and the coherent laser equations. F.M. and W.B. did most of the numerical simulations. E.G. and G.L.C. directed the research. All authors contributed to writing of the manuscript.

[1] T. Ritz, S. Adem, and K. Schulten, Biophysical Journal **78**, 707 (2000).

[2] C. T. Rodgers and P. J. Hore, Proceedings of the National Academy of Sciences **106**, 353 (2009).

[3] E. M. Gauger, E. Rieper, J. J. Morton, S. C. Benjamin, and V. Vedral, Physical Review Letters **106**, 040503 (2011).

[4] H. G. Hiscock, S. Worster, D. R. Kattnig, C. Steers, Y. Jin, D. E. Manolopoulos, H. Mouritsen, and P. Hore, Proceedings of the National Academy of Sciences **113**, 4634 (2016).

[5] J. Strümpfer, M. Sener, and K. Schulten, the Journal of Physical Chemistry Letters **3**, 536 (2012).

[6] M. K. Şener, J. D. Olsen, C. N. Hunter, and K. Schulten, Proceedings of the National Academy of Sciences **104**, 15723 (2007).

[7] J. T. Beatty, J. Overmann, M. T. Lince, A. K. Manske, A. S. Lang, R. E. Blankenship, C. L. Van Dover, T. A. Martinson, and F. G. Plumley, Proceedings of the National Academy of Sciences **102**, 9306 (2005).

[8] S. Baghbanzadeh and I. Kassal, the Journal of Physical Chemistry Letters **7**, 3804 (2016).

[9] S. Baghbanzadeh and I. Kassal, Physical Chemistry Chemical Physics **18**, 7459 (2016).

[10] N. R. Council, *Advancing Land Change Modeling: Opportunities and Research Requirements* (The National Academies Press, Washington, DC, 2014).

[11] T. Yabe, T. Ohkubo, S. Uchida, K. Yoshida, M. Nakatsuka, T. Funatsu, A. Mabuti, A. Oyama, K. Nakagawa, T. Oishi, *et al.*, Applied Physics Letters **90**, 261120 (2007).

[12] S. Uchida, T. Yabe, Y. Sato, K. Yoshida, A. Ikesue, T. Ohkubo, A. Mabuchi, Y. Ogata, K. Nakagawa, A. Ohyama, *et al.*, in *AIP Conference Proceedings*, Vol. 830 (American Institute of Physics, 2006) pp. 439–446.

[13] D. Graham-Rowe, Nature Photonics **4**, 64 (2010).

[14] P. D. Reusswig, S. Nechayev, J. M. Scherer, G. W. Hwang, M. G. Bawendi, M. A. Baldo, and C. Rotschild, Scientific Reports **5**, 14758 (2015).

[15] X. Hu, T. Ritz, A. Damjanovi, and K. Schulten, the Journal of Physical Chemistry B **101**, 3854 (1997).

[16] X. Hu, A. Damjanović, T. Ritz, and K. Schulten, Proceedings of the National Academy of Sciences **95**, 5935 (1998).

[17] G. S. Engel, T. R. Calhoun, E. L. Read, T.-K. Ahn, T. Mančal, Y.-C. Cheng, R. E. Blankenship, and G. R. Fleming, Nature **446**, 782 (2007).

[18] G. Panitchayangkoon, D. Hayes, K. A. Fransted, J. R. Caram, E. Harel, J. Wen, R. E. Blankenship, and G. S. Engel, Proceedings of the National Academy of Sciences **107**, 12766 (2010).

[19] J. Grad, G. Hernandez, and S. Mukamel, Physical Review A **37**, 3835 (1988).

[20] F. C. Spano and S. Mukamel, the Journal of Chemical Physics **91**, 683 (1989).

[21] G. L. Celardo, F. Borgonovi, M. Merkli, V. I. Tsifrinovich, and G. P. Berman, the Journal of Physical Chemistry C **116**, 22105 (2012).

[22] D. Ferrari, G. Celardo, G. P. Berman, R. Sayre, and F. Borgonovi, the Journal of Physical Chemistry C **118**, 20 (2014).

[23] M. Gullì, A. Valzelli, F. Mattiotti, M. Angeli, F. Borgonovi, and G. L. Celardo, New Journal of Physics **21**, 013019 (2019).

[24] P. R. Patlolla, A. D. Mahapatra, S. S. Mallajosyula, and B. Datta, New Journal of Chemistry **42**, 6727 (2018).

[25] M. Caselli, L. Latterini, and G. Ponterini, Physical Chemistry Chemical Physics **6**, 3857 (2004).

[26] V. Gavrilenko and M. Noginov, the Journal of Chemical Physics **124**, 044301 (2006).

[27] N. J. Hestand and F. C. Spano, Chemical Reviews **118**, 7069 (2018).

[28] M. O. Scully, Physical Review Letters **104**, 207701 (2010).

[29] K. E. Dorfman, D. V. Voronine, S. Mukamel, and M. O. Scully, Proceedings of the National Academy of Sciences **110**, 2746 (2013).

[30] M. O. Scully, K. R. Chapin, K. E. Dorfman, M. B. Kim, and A. Svidzinsky, Proceedings of the National Academy of Sciences **108**, 15097 (2011).

[31] C. Creatore, M. A. Parker, S. Emmott, and A. W. Chin, Physical Review Letters **111**, 253601 (2013).

[32] A. Fruchtman, R. Gómez-Bombarelli, B. W. Lovett, and E. M. Gauger, Physical Review Letters **117**, 203603 (2016).

[33] K. Higgins, S. Benjamin, T. Stace, G. Milburn, B. W. Lovett, and E. Gauger, Nature Communications **5**, 1 (2014).

[34] Y. Zhang, S. Oh, F. H. Alharbi, G. S. Engel, and S. Kais, Physical Chemistry Chemical Physics **17**, 5743 (2015).

[35] W. M. Brown and E. M. Gauger, the Journal of Physical Chemistry Letters **10**, 4323 (2019).

[36] J. Gierschner, S. Varghese, and S. Y. Park, Advanced Optical Materials **4**, 348 (2016).

[37] S. Özçelik, I. Özçelik, and D. L. Akins, Applied Physics Letters **73**, 1949 (1998).

[38] J. C. Hindman, R. Kugel, M. R. Wasielewski, and J. J. Katz, Proceedings of the National Academy of Sciences **75**, 2076 (1978).

[39] L. M. Günther, M. Jendrny, E. A. Bloemsma, M. Tank, G. T. Oostergetel, D. A. Bryant, J. Knoester, and J. Köhler, the Journal of Physical Chemistry B **120**, 5367 (2016).

[40] G. Celardo, M. Angeli, T. Craddock, and P. Kurian, New Journal of Physics **21**, 023005 (2019).

[41] F. C. Spano and S. Mukamel, the Journal of Chemical Physics **91**, 683 (1989).

[42] Closely spaced molecules require a modification of the dipole interaction term which is then not solely determined by the TDM [15, 16].

[43] H. P. Breuer and F. Petruccione, *The theory of open quantum systems* (Oxford University Press, Great Clarendon Street, 2002).

[44] V. N. Shatokhin, M. Walschaers, F. Schlawin, and A. Buchleitner, New Journal of Physics **20**, 113040 (2018).

[45] Y. Zhang, G. L. Celardo, F. Borgonovi, and L. Kaplan, Physical Review E **95**, 022122 (2017).

[46] T. G. Pavlopoulos, Progress in Quantum Electronics **26**, 193 (2002).

[47] P. Würfel and U. Würfel, *Physics of solar cells: from basic principles to advanced concepts* (John Wiley & Sons,

2016).

[48] A. P. Deshmukh, D. Koppel, C. Chuang, D. M. Cadena, J. Cao, and J. R. Caram, the Journal of Physical Chemistry C **123**, 18702 (2019).

[49] M. O. Scully and M. S. Zubairy, *Quantum optics* (American Association of Physics Teachers, 1999).

[50] S. Zhu, M. Scully, H. Fearn, and L. Narducci, Zeitschrift für Physik D Atoms, Molecules and Clusters **22**, 483 (1992).

[51] X. Hu and K. Schulten, Biophysical Journal **75**, 683 (1998).

[52] X. Hu, T. Ritz, A. Damjanović, F. Autenrieth, and K. Schulten, Quarterly Reviews of Biophysics **35**, 1 (2002).

[53] The case of a black body pumping at $T_{BB} = 3000$ K is discussed in the SI.

[54] J. Yao, X. Yang, X. Yin, G. Bartal, and X. Zhang, Proceedings of the National Academy of Sciences **108**, 11327 (2011).

[55] R.-M. Ma and R. F. Oulton, Nature Nanotechnology **14**, 12 (2019).

[56] J. Huh, S. K. Saikin, J. C. Brookes, S. Valleau, T. Fujita, and A. Aspuru-Guzik, Journal of the American Chemical Society **136**, 2048 (2014).

[57] K. Amarnath, D. I. Bennett, A. R. Schneider, and G. R. Fleming, Proceedings of the National Academy of Sciences **113**, 1156 (2016).